Uzbek Journal of Physics

Vol.20(№4) 2018 PP.265-274

THE COLLIDING PARTICLES MASS RATIO INFLUENCE ON PECULIARITIES OF LOW-ENERGY ION NEAR-SURFACE IMPLANTATION AT CHANNELING CONDITIONS

F.F. Umarov[1], A.M. Rasulov[2], A.A. Dzhurakhalov[3]

[1]Kazakh-British Technical University, Tole be Str.59, 050000, Almaty, Kazakhstan
[2]Tashkent University of Information Technologies, Ferghana branch, Mustaqillik Str. 185, 150118 Ferghana, Uzbekistan
[3]University of Antwerpen, Middelheimlaan 1, BE-2020 Antwerpen, Belgium

Si(110) ва SiC(110) монокристалларида E_0=1–5 кэВ бошланғич энергияли каналланган P^+ ионлари имплантацияси ва турли массали ионларнинг ўзаро таъсирининг улар профил тақсимоти ва энергия йўқотишларига боғлиқлиги ҳамда GaAs(100) монокристалл сиртига 1 кэВ энергияли Be^+, Se^+ ионларининг ва Cu(001) монокристалл сиртига 5 кэВ энергияли Ar^+, Kr^+ ионларининг сирпаниш бурчаги остида тушиши жараёнининг жуфт тўқнашишларга асосланган компьютер модели ёрдамида тадқиқ этилган. Тадқиқот натижалари шуни кўрсатдики, параксиал қисмдаги энергия йўқотишларнинг асосий сабаби, ноэластик энергия йўқотишлардан келиб чиқади. Каналланган ионларнинг юпқа монокристаллардан ўтишида йўқотиладиган энергияси ва кристалл чуқурлиги бўйича профил тақсимоти каналнинг ўлчамига ҳамда тўқнашувчи атомларнинг массалари нисбатига боғлиқлиги кўрсатилган. Сиртга яқин қатламда каналланган Se^+ ионларининг профил тақсимоти чўққиси жуда тор ва югуриш йўли қисқа ҳамда каналланган чўққининг ярим кенглиги Be^+ ионикига нисбатан тор бўлиши кўрсатилган. Олинган натижалар кристалнинг сиртига яқин қатламларида каналланган ионларнинг профил тақсимотини талаб даражасидаги формасини олишнинг оптимал шартини яратиш имкониятини беради.

С помощью компьютерного моделирования в приближении парных столкновений исследованы особенности ионной имплантации и влияния соотношения масс сталкивающихся частиц на пробеги, потери энергии и профили распределения ионов P^+ с энергиями 1–5 кэВ, каналированных в Si(110) и SiC(110) при нормальном падении, а также ионов Be^+ и Se^+ с энергией 1 кэВ в GaAs(100) и ионов Ar^+ и Kr^+ с энергией 5 кэВ в Cu(001) монокристаллах при скользящем падении. Показано, что для параксиальной части пучка основной вклад в полные потери энергии вносят неупругие потери энергии. Потери энергии ионов, прошедших сквозь тонкие кристаллы, и профили распределения ионов по глубине зависят от ширины канала и соотношения масс сталкивающихся атомов. Показано, что в условиях скользящего поверхностного каналирования ионов Se^+ основной пик имплантированного профиля распределения существенно сужен и пробеги неглубокие и полуширина профиля для этих ионов уже, чем для ионов Be^+. Полученные результаты позволяют выбирать оптимальные условия для получения профилей распределения с требуемой формой в приповерхностной области кристалла.

In the present work the peculiarities of ion implantation and colliding particles mass ratio influence on the ranges, energy loss and profiles of distribution for 1–5 keV P^+ ions channelling in Si(110) and SiC(110) at normal incidence, and 1 keV Be^+ and Se^+ ions in GaAs(100), as well as 5 keV Ar^+ and Kr^+ on Cu(001) surface at glancing incidence are carried out by computer simulation in binary collision approximation. It is shown that for paraxial part of a beam the main contribution to the total energy loss comes from inelastic ones. It has been established that the energy loss of ions transmitted through thin crystal and depth profile distributions depend on width of the channel and mass ratio of colliding atoms. It was shown that at grazing surface channeling conditions the main peak of the implanted depth distributions is considerably shallow, the range for Se^+ ions is shallower and the half-width of profile for these ions is narrow than that for Be^+ ions. The results allow one to select the optimum for implanted depth distributions with demanded shape at narrow near-surface area of crystals obtaining.

I. INTRODUCTION

Ion implantation has become a very important technique for modifying surface and impurity doping of semiconductors [1-7]. The ion implantation processes lead to change of a profile of composition and structure of the subsurface layers. Using glancing-angle ion implantation for surface modification rather than conventional near-normal incidence ions allows one to expand the energy range up to ~10 keV and has the advantages of reducing damage (such as crater formation) and preferentially removing surface asperities leading to flat surfaces. This is due to the peculiarities of sputtering processes at grazing incidence. Channeling of low-energy ions in metal and semiconductor single crystals offers the opportunity to create the method of local ion implantation in ultrathin film nanotechnology and surface nanoengineering. Therefore ranges, energy loss and profiles of distribution of low-energy ions channeling in crystals have received considerable experimental and theoretical interest [6-12]. In the present work for revealing of the influence of colliding particles mass ratio μ (where $\mu = m_2/m_1$ is the mass ratio of target atom and ion, respectively) on the ranges, energy loss and profiles of distribution the channelling of 1–5 keV P^+ ions in Si(110) and SiC(110) at normal incidence and 1 keV Be^+ and Se^+ ions in GaAs(100) at glancing incidence is carried out by computer simulation in binary collision approximation. The μ values for P^+ ions colliding with Si and C target atoms are equal to 0.9 and 0.39, correspondingly, ($\mu<1$: inverse mass ratio), for Be^+ ions colliding with Ga and As atoms are equal to 7.74 and 8.31, correspondingly, ($\mu>1$: direct mass ratio) and for Se^+ colliding with Ga and As target atoms 0.88 and 0.95, correspondingly, ($\mu<1$: inverse mass ratio). Si, SiC and GaAs crystals have a great importance because of their use in semiconductor technologies. Especially, silicon carbide exhibits a large band gap, a higher break down field, a higher thermal conductivity, and a higher saturation velocity, compared to widely used silicon. Now β-SiC(110) is widely used as an heterogeneous catalyst. The (100) surface of GaAs semiconductor is one of the most widely used surface in both homo- and heteroepitaxial growth for the manufacturing of electronic devices. Implantation of Be and Se into GaAs allows one to make the acceptor and donor impurities in this semiconductor. For small crystal depths the approaches which are used in the analytical theory of orientation effects on the large depths, become unacceptable and a computer simulation methods for the channeling process modeling appear to be the most preferable [5, 7, 9-14]. So the theoretical investigation of atomic collision processes in crystals caused by particle irradiation and deposition is usually done using computer simulation because real physical conditions (e.g. complicated interatomic interaction potential, surfaces, interfaces, defects) can be taken into account much easier than it possible by using analytical methods [5, 7, 13, 14-17].

II. COMPUTER SIMULATION METHOD

The channeling simulation program used in the present work is similar by structure to the well-known MARLOWE program and based on the binary collision approximation with two main assumptions: (i) only binary collisions of ions with target atoms or between two target atoms are considered; and (ii) the path which a projectile goes between collisions is represented by straight-line segments [5, 7]. In the binary collision model particles move along straight-line segments, representing asymptotes to their trajectories in laboratory system and one determines not a particle trajectory but rather the

difference between the angles characterizing the initial and final directions of motion. While this approach permits one to cut the required computer time (compared with direct integration of the equations of motion), it also entails a systematic error due to the fact over short segments of path, the real ion trajectory differs from the asymptotes used to replace the former. This error was estimated in [18] for the Cu-Cu pair, a number of potentials and three values of energy. It was established that the deviation of an asymptote from the real trajectory is essential only for head-on collision and high energies.

For the particles interaction description the Biersack-Ziegler-Littmark potential [4] with regard to the time integral was used. The BZL approximation for the screening function in the Thomas-Fermi potential takes into account the exchange and correlation energies and the so-called "universal" potential, obtained in this way shows good agreement with experiment over a wide range of interatomic separations. Trajectories of P^+ ions in Si(110) and SiC(110) targets at normal incidence and Be^+ and Se^+ ions in GaAs(100) at glancing incidence have been computer simulated with regard to elastic and inelastic energy loss. Elastic and inelastic energy loss have been summed along trajectories of scattered ions. The inelastic energy loss ε (E_0, p) was regarded as local depending on the impact parameter p and included into the scattering kinematics. These loss have been calculated on the basis of Firsov model modified by Kishinevsky [7] and contain direct dependence on impact parameter:

$$\varepsilon(E_0, p) = \frac{0.3\times10^{-7}\nu_1 Z_1 (Z_1^{1/2}+Z_2^{1/2})(Z_1^{1/6}+Z_2^{1/6})}{\left[1+\dfrac{0.67\sqrt{Z_1}r_{\min}}{a_{\text{ТФ}}(Z_1^{1/6}+Z_2^{1/6})}\right]^3}\left[1-0.68\frac{V(r_{\min})}{E_r}\right],$$

where v and E_r are the velocity and energy of relative atomic motion, Z_1 is a greater, and Z_2 is the smaller of the atomic numbers, and r_0 is in units of Å.

The expressions for the ion E_i and recoil E_r energies after binary collision taking into account inelastic loss can be written as follows [19]:

$$E_i = \frac{E_0}{(1+\mu)^2}(\cos\theta_i \pm \sqrt{f\mu^2 - \sin^2\theta_i})^2,$$

$$E_r = \frac{\mu}{(1+\mu)^2}E_0(\cos\theta_r \pm \sqrt{f^2 - \sin^2\theta_r})^2.$$

where $f = [1-(1+\mu)/\mu\varepsilon(E_0,p)/E_0]$; θ_i and θ_r – the angles of ion and recoil scattering in the laboratory system of coordinate; E_0 – initial energy of impinging ion; p – impact parameter and $\mu = m_2/m_1$.

In [19] the dependencies of $\varepsilon(E_0, p)$ on the basis of the Firsov, Kishinevsky [7] and Oen-Robinson [20] models for $Ne^+ \rightarrow Ni$ pair and low energy E_0=1–10 keV has been calculated. Estimating the accuracy of models for various values of the impact parameter in the low energy range, it is necessary to notice that in a small impact parameters region (p<0.5 Å) it is more preferable to use the Kishinevsky model, however in the region of large impact parameters all three models give approximately the same results and they are useful even when the energy E_0~100 eV. Above mentioned models were checked experimentally more than once. One the whole, experimental data agree well with these theories, however in some cases the calculated values exhibit discrepancies from the measurement which reach 30–40% [21, 22].

But in the case of the solid phase, the binary interaction gets distorted by the influence of neighboring atoms and multiple collisions. It is impossible to calculate inelastic energy loss in this case without exact knowledge of the trajectory of scattering ions. For their calculation it is necessary to perform computer simulation of ion scattering and channeling in the single crystal.

A parallel, uniform, monoenergetic ion beam impinges on an impact area on a surface of a crystal. The angle of incidence of primary ions ψ was counted from a target surface. It is assumed that the incident beam is of small density, so the ions of the beam do not hit twice at the same place. The impact area covers an elementary cell in the transverse plane of channel axis. The number of incident particles is 4×10^4. In simulation the crystal lattice of Si and SiC was the same as a diamond cubic structure, with zincblende lattice for SiC. The structure of Cu was a face-centered cubic lattice. The shape of the target area is chosen such that by translating it, one could cover the entire surface of the crystal. Successive multiply scattering of ions from atoms in the rows lying along the principal crystallographic axes is followed in a special search procedure to find the next lattice atom or atoms with which the projectile will interact with impact parameters for all target atoms forming the walls of a channel calculated for each layer in the crystallite. Around the colliding target atom, the coordinates of the nearest neighbor atoms are consistently set according the crystal structure of the target. For each set of atoms the following conditions are checked: (i) it should be at the front part of the ion movement relatively to a crossing point of asymptotes of the projectile movement directions before and after collision; (ii) the ion impact parameter should be less than p_{lim} (p_{lim} is the impact parameter corresponding to the scattering angle of 0.05°); (iii) among colliding atoms, it should be the first in turn p_1, p_2, p_3… on the consecutive collisions. After each collision the scattering angle, energy and the new movement direction of channeled ion are determined. It is checked if the projectile is still moving in the given channel. The coordinates of dechanneling are used to obtain the dechanneled and channeled fractions as function of the depth. The incident ions were followed throughout their slowing-down process until their energy fall below 25 eV.

In order to consider simultaneous and nearly simultaneous collisions of a particle with the atoms of the adjacent chains, the special procedure proposed in [18] was used. So-called simultaneous collisions which occur if a projectile has a symmetrical position, and can collide with more than one target atom at the same time, are approximated by successive binary collisions. The inclusion of the thermal vibrations assumed that the target atoms oscillated independently of one another, and their deflections from the equilibrium position are subject to the normal Gaussian distribution. The effect of correlation is equivalent to a reduction of the vibration amplitude of about 5–10% depending on the effect being looked at [23].

The program allowed the consideration of main peculiarities in channeled particle distribution with depth, such as collision-by-collision details of trajectories, flux-peaking and difference in specific energy loss for random and channeled trajectories. The method is described in detail in [7, 11, 14].

III. RESULTS AND DISCUSSION

By computer simulation it has been observed in details the dynamics of the change of the character of trajectories, the ranges, energy loss and profiles of distribution of P^+ ions in thin Si(110) and SiC(110) crystals and Be^+ and Se^+ ions in GaAs(100) crystal, as

well as the angular and energy distributions of ions transmitted through thin crystals versus the composition of single crystal, initial energy and impact parameters from the center of the channel. The channeling effect in the case of inverse mass ratio of colliding particles manifests itself in a number of features associated with the existence of a limiting scattering angle $\theta_{lim}=\arcsin\mu$ in a single collision, as well as with the fact that scattering at a given angle $\theta<\theta_{lim}$ is possible for two values of impact parameter p [7]. Therefore, the scattered ion energy is a double-valued function of the scattering angle. Figure 1 presents dependences of the energy E retained by the Kr^+ ions scattered from copper atomic rows on the scattering angle θ for ψ=17.5 and 22.5°.

The broken curve shows a similar dependence for single scattering. In this case the $\mu\approx0.758$, $\theta_{lim}\approx49.3°$, and $p_{lim}\approx0.10$ Å. A trajectory analysis revealed that for small grazing angles (in the $Kr^+\rightarrow Cu$ case, up to ψ=20°) and for μ<1, the usual atomic row effect is observed, just as in the case μ>1. Indeed, for ψ=17.5° one observes a double-valued dependence $E(\theta)$ caused by the conventional quasisingle (branch 2: QS) and quasidouble (branch 3:QD) scattering, as well as blocking on the sides of small and large scattering angles, Note that for small ψ the scattering angles in the case of an atomic row are smaller than θ_{lim} for a single collision, the ions do not approach close enough the atoms in the row, and the impact parameters $p_i>p_{lim}$. As shown on the right of Fig. 1, one observes in this case the usual behavior of $\theta(p)$ dependence. As the grazing angle increases (ψ=22.5°) small impact parameters $p_i<p_{lim}$ for which the $\theta(p)$ dependence reverses its course become accessible, adding new types of trajectories (*1*, *4*, *5*) to the conventional ones, QS and QD (*2*, *3*), which results in a substantial change of the $E(\theta)$ behavior. Trajectory *1* corresponds to QS scattering with an impact parameter in the principal collision $p<p_{lim}$, trajectory *4* to QD scattering with an impact parameter in one or two strong collisions $p<p_{lim}$ and trajectory *5* to multiple scattering with $p<p_{lim}$ in one or several collisions. A specific feature of the atomic row effect in this case is the appearance of additional branches (*1*, *4*, *5*) in the $E(\theta)$ dependence, which should result in the formation, in the energy spectrum of scattering at angles θ close to θ_{lim} of three peaks in the low energy part, as well as in scattering at angles θ considerable in excess of θ_{lim}.

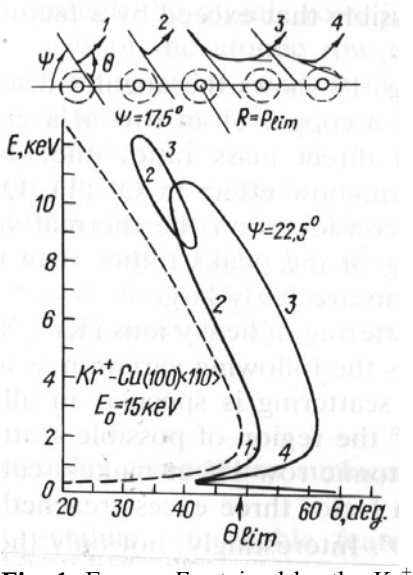


Fig. 1. Energy E retained by the Kr^+ ions scattered from copper atom rows vs the scattering angle θ for ψ=17.5 and 22.5°.

It has been established that for a paraxial part of a channeled beam the contribution of inelastic energy loss to the total energy loss in the entire energy interval (1–5 keV) is a main both for direct and inverse mass ratio of colliding particles [10].

The energy distributions of 3 keV P^+ ions transmitted through thin (ΔZ=50 nm) Si(110) and SiC(110) crystals at the channeling conditions have been calculated and studied as function of the crystal geometrical structure (Fig. 3). The lattice parameter for

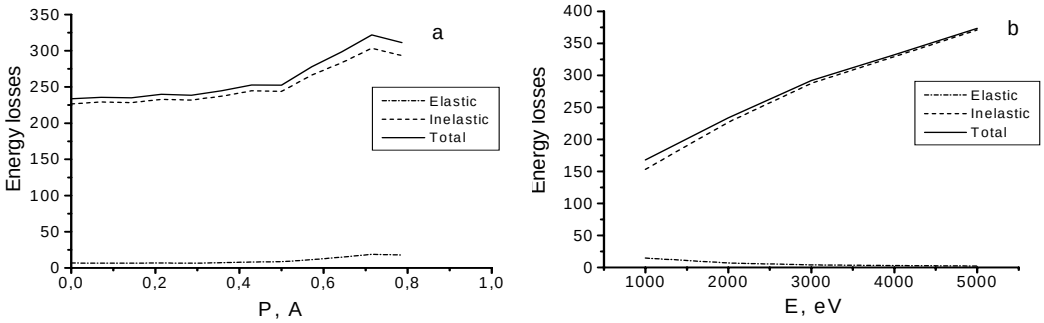


Fig. 2. Energy loss of P^+ ions transmitted through thin (*dZ*=500 Å) Si (110) film versus the impact parameter counted from the centre of channel <110> at E = 2 keV (*a*) and versus the initial energy for central particle (*b*).

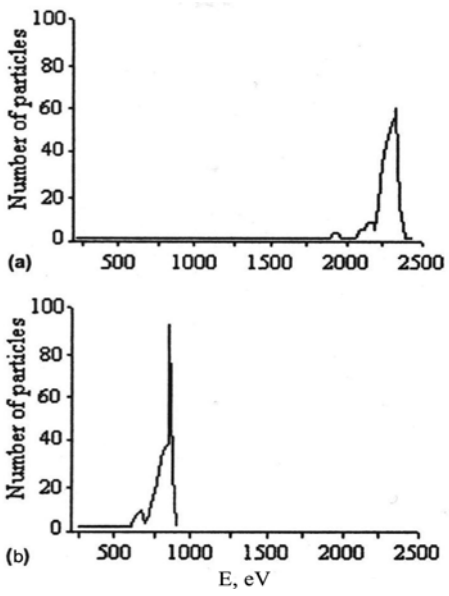


Fig. 3. Energy distributions of 3 keV P^+ ions transmitted through Si(110) (*a*) and SiC(110) (*b*) crystal films with thickness ΔZ = 50 nm in the <110> direction.

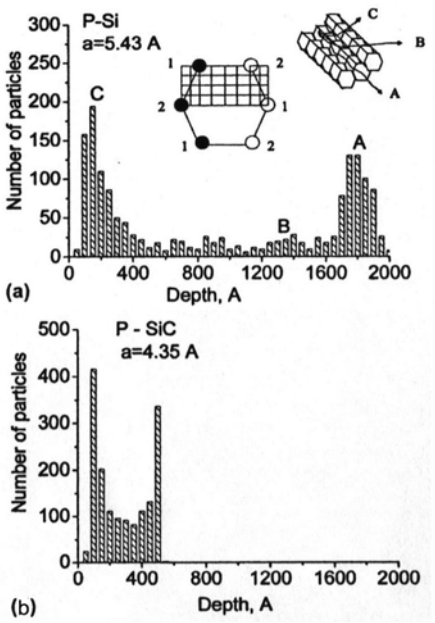


Fig. 4. Depth profile distributions of implanted particles at 3 keV P^+ ions bombardment along the <110> direction of Si(110) (*a*) and SiC(110) (*b*).

Si single crystal is 0.543 nm and for SiC single crystal is 0.435 nm. The crystal structure for these crystals looks like as a diamond structure [24, 25].

It has been established that for two targets the energy distributions of transmitted ions consist of one distinguishable peak corresponding to the ion channeling conditions, but in the case of SiC target the energy distribution becomes more narrow and the energy of transmitted ions is very low due to decreasing the lattice parameter and inverse mass ratio influence in comparison of one for Si target.

To take into account the influence of channeling on a depth profile of implanted ions is a complex problem. In the case of amorphous solids a depth profile is a Gaussian

distribution caused by a randomize character of particles collisions. In the single crystal case the total depth profile distribution is formed by three components of ion beam: a chaotic part of a beam, a planar channeling part and an axial channeling part.

The calculated depth profiles of implanted particles at 3 keV P^+ ions bombardment along the <110> direction of Si(110) and SiC(110) consist of two peaks: a non-channeled peak near the surface region and channeled peak deeper in the layers (Fig. 4). The labels A, B and C in the distribution correspond to the trajectories of ions in axial channeling (A), planar channeling (B) and disordered motion (C) (see, insert of Fig. 2*a*). It is seen that the axial channeling flux forms the distinguished peak near the maximal depth penetration. The comparison of these results shows that the ion range and the maximal depth of profile distribution decrease with decreasing the lattice parameter and mass of target atoms ($m_C<m_{Si}$). Therefore, in the SiC case the half width of channeled peak is narrow, this peak and the maximal depth of profile distribution are significantly shifted to the shallower region, the intensity of both non-channeled and channeled peaks increase sharply.

In the case of Be^+ and Se^+ ions bombarded the GaAs(100) surface at grazing incidence the ions move in the surface semichannels and channels which is parallel to the surface and transfer the small portions of their energy to a great number of atoms which form of channels and semichannels walls. The number of 1 keV Be^+ and Se^+ ions implanted into GaAs(100) surface versus the incidence angle Ψ for <110> and <$\bar{1}$10> directions has been calculated (Fig. 5).

The number of implanted Se^+ ions is much greater than the number of Be^+ ions. At the angles of incidence where the minimum of the dependence is observed (Fig. 3*b*) the incident ions are intensively reflected by surface semichannels because of the ion focusing effect [9].

It is established that some difference of these dependencies is explained by different shapes of surface semichannels in these directions. It is clear that at grazing angles smaller than some critical angle, ion implantation does not take place. The value of the critical angle decreases with mass of incident ion decreasing. The inverse mass ratio of colliding particles in case of Se^+ ions is lead to considerable increase of incidence angle Ψ_{in} from which the ions penetration into GaAs surface layers are begin in comparison with Be^+ ions (for <110> direction: $\Psi_{inBe} = 10°$ and $\Psi_{inSe} = 18°$).

Figure 6 shows implanted depth distributions of 1 keV Be^+ and Se^+ ions

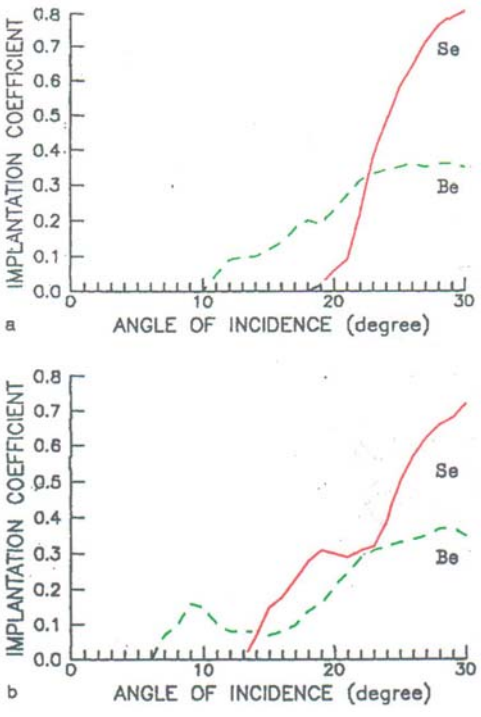


Fig. 5. Number of 1 keV Be^+ and Se^+ ions implanted into GaAs(100) surface versus the incidence angle Ψ for <110> and <$\bar{1}$10> directions.

for <Ī10> direction calculated for three incidence angles values. The oscillatory behavior of depth distributions is explained by shape of channel in the <Ī10> direction. At grazing incidence the primary beam ions penetrates in several nearest to surface atomic layers during the process of their movement in channels of low index directions along the surface. Therefore, in this case the main peak of the implanted depth distributions is considerable shallow. Note that 1 layer is 0.136 nm. The implanted depth profiles depend on the mass ratio of colliding particles, the crystal orientation and the angle of incidence. At $\psi = 30°$ the depth profile for Se^+ ions is slightly shifted in the deep layers region (Fig. 4*b*). The comparison of calculated depth distributions for Be^+ and Se^+ ions shows that the range for Se^+ ions is shallower than that for Be^+ ions and the half-width of profile for Se^+ is narrow, because the small mass and size of Be^+ ions allows them to penetrate into deep layers region.

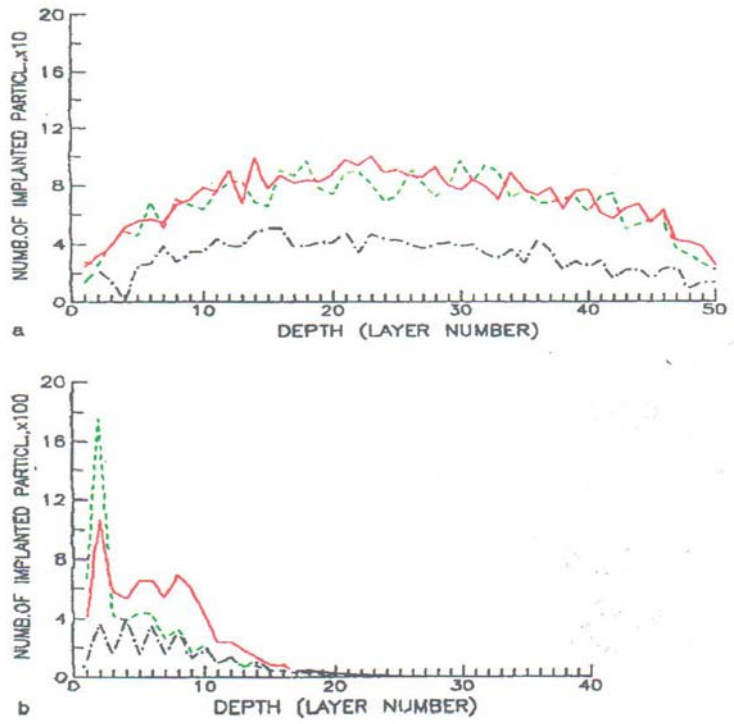


Fig. 6. Implanted depth distributions of 1 keV Be^+ (*a*) and Se^+ (*b*) ions for <Ī10> direction at $\psi = 19°$ (dash-dott), 26° (dash) and 30° (solid line).

In Fig. 7 the depth distributions of 5 keV Ar^+ (*a*) and Kr^+ (*b*) ions implanted into Cu(001) <110> surface have been presented for three values of angle of incidence. It is clear that the implanted depth distributions of bombarded particles contain a maximum. With the angle of incidence ψ increasing the maximum of distribution is slightly shifted on the field of deep layers and a half-width of distribution increases. In a case of Kr ions ($\mu \approx 0.76$: inverse mass ratio of colliding particles) for the incidence angle range up to ψ=16°, the main part of implanted ions is arranged in four-fife layers nearest to the surface. The calculated results show that at ion bombardment of Cu(001) surface along a

<110> directions the ions are implanted much more deeply due to planar channeling and their depth distributions have not a sharp maximum in the near surface area.

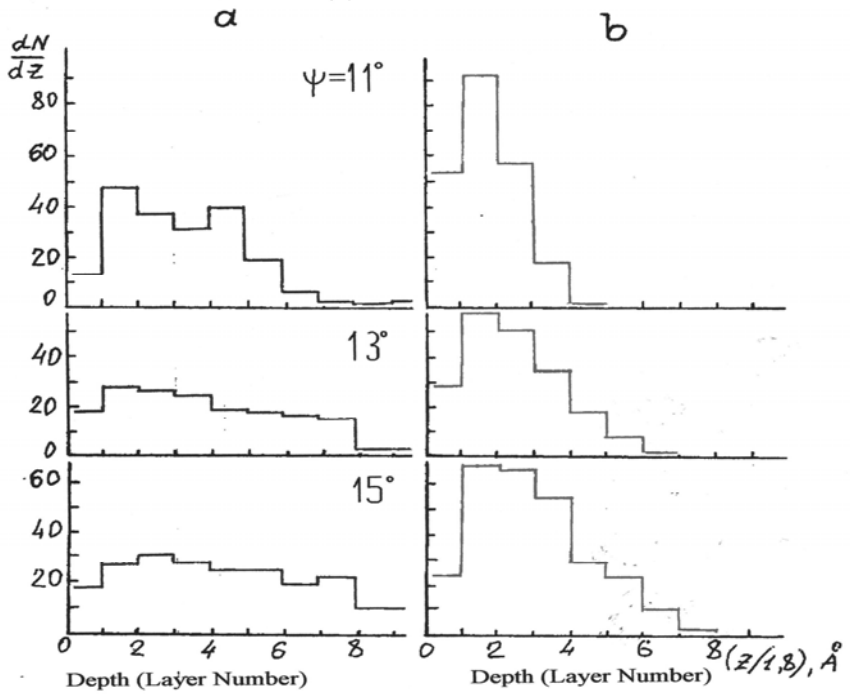


Fig. 7. Depth distributions of 5 keV (*a*) Ar^+ and (*b*) Kr^+ ions implanted into Cu(001) <110> surface at various grazing angles. Note that 1 layer is 1.81 Å.

IV. CONCLUSION

The obtained results are illustrated the inverse mass ratio effect on ranges, energy loss and profiles of distribution of low-energy ions channeled in thin semiconductor crystals at normal and grazing incidence on their surface. It is shown that for the paraxial part of a beam the main contribution to the total energy loss comes from inelastic energy loss. The presence of heavy atoms in lattice leads to dechanneling of the part of paraxial beam and to decrease of the ion ranges. The characteristics of particles transmitted through the thin single crystal films and implanted into crystals both at the normal and grazing incidence on the surface are sensitive to the mass ratio of colliding particles and width of channel. It was shown that in case of Be^+ and Se^+ ions implantation into GaAs(001) the main peak of the implanted depth distributions is considerable shallow, the range for Se is shallower and the half-width of profile for Se^+ is narrow than that for Be^+ ions. The obtained results allow one to selecting the optimum for implanted depth distributions with demanded shape in narrow near-surface area (5–10 atomic layers) of crystals production.

Acknowledgements. The authors would like to thank Drs. Umarov T.F. and Khaidarov A.Kh. for very useful help.

REFERENCES

1. M.A. Van Hove, Surf. Sci. **603**, 1301 (2009).

2. Ion Implantation: Equipment and Techniques. Eds. H. Ryssel, Glawischnig (Springer-Verlag, Berlin, 1983).
3. Channeling: Theory, Observation and Applications. Ed. D.V. Morgan (Wiley & Sons, London, New York, 1973).
4. J.F. Ziegler, J.P. Biersack, U. Littmark. The Stopping and Ranges of Ions in Solids (Pergamon Press, New York, 1985).
5. W. Eckstein. Computer Simulation of Ion-Solid Interaction (Springer, Heidelberg, 1991).
6. E.S. Mashkova, V.A. Molchanov. Medium-energy Ion Reflection from Solids (Amsterdam, North-Holland, 1985).
7. E.S. Parilis, L.M. Kishinevsky, N.Yu. Turaev, B.E. Baklitsky, F.F. Umarov, V.Kh. Ferleger, S.L. Nizhnaya, I.S. Bitensky. Atomic Collisions on Solid Surfaces (Amsterdam, North-Holland, 1993).
8. R.G. Wilson, J. Appl. Phys. **60**, 2797 (1986).
9. A.A. Dzhurakhalov, I.I. Khafizov, Nucl. Instr. Meth. Phys. Res. B **153**, 326 (1999).
10. F.F. Umarov, A.M. Rasulov, A.Kh. Khaidarov, Rad. Eff. & Defects in Solids **158**, 481 (2003).
11. A.A. Dzhurakhalov, F.F. Umarov, Nucl. Instr. Meth. Phys. Res. B **136-138**, 1092 (1998).
12. F.F. Umarov, A.M. Rasulov, Appl. Surf. Sci. **135**, 269 (1998).
13. F.F. Umarov, A.A. Dzhurakhalov, Surface and Interface Analysis **45**(1), 83 (2013).
14. F.F. Umarov, A.A. Dzhurakhalov. Computer Simulations: Technology, Industrial Applications and Effects on Learning (The chapter in the book) **(**Nova Sciences Publishers, Inc. NY, USA, 2013).
15. K. Gartner, D. Stock, C. Wende, and M. Nitschke, Nucl. Instr. Meth. Phys. Res. B **90**, 124 (1994).
16. M. Rosselt, K.-H. Heinig, Nucl. Instr. Meth. Phys. Res. B **102**, 236 (1995).
17. Rongbin Li, Yongbin Dai, Xiaojun Hu, Heshen Sheng, Xianchang He, Nucl. Instr. Meth. Phys. Res. B **211**, 91 (2003).
18. M.T. Robinson, I.M. Torrens, Phys. Rev. B **9**, 5008 (1974).
19. F.F. Umarov, N. Narkulov, F.B. Abdulkasymov, Nucl. Instr. Meth. Phys. Res. B **164-165**, 656 (2000).
20. S. Oen, M.T. Robinson, Nucl. Instr. Meth. B **132**, 647 (1976).
21. K.J. Snowdon, D.J. O'Connor, and R.J. McDonald, Radiat. Eff. and Defects in Solids **109**, 33 (1989).
22. R. Monreal, F. Flores, A. Naermann, W. Heiland, and S. Schubert, Radiat. Eff. and Defects in Solids **109**, 75 (1989).
23. J.H. Barret and D.P. Jackson, Nucl. Instr. Meth. B **170**, 115 (1980).
24. A.M. Rasulov, A.A. Dzhurakhalov, F.F. Umarov, Sh.D. Sultonov, A. Khaidarov, Proc. of SPIE **5974**, 597401-2 (2004).
25. A.M. Rasulov, A.A. Dzhurakhalov, Computational Material Science **33**, 148 (2005).

.